

# Effect of Axial Ligands on the Molecular Configurations, Stability, Reactivity, and Photodynamic Activities of Silicon Phthalocyanines

Liqiang Luan, Lanlan Ding, Jiawei Shi, Wenjuan Fang, Yuxing Ni, and Wei Liu\*<sup>[a]</sup>

**Abstract:** To demonstrate the effect of axial ligands on the structure–activity relationship, a series of axially substituted silicon phthalocyanines (SiPcs) have been synthesized with changes to the axial ligands. The reactivity of the axial ligand upon shielding by the phthalocyanine ring current, along with their stability, photophysical, and photodynamic therapy (PDT) activities were compared and evaluated for the

first time. As revealed by single-crystal XRD analysis, rotation of the axial –OMe ligands was observed in SiPc **3**, which resulted in two molecular configurations coexisting synchronously in

**Keywords:** photochemistry · phthalocyanines · silicon · structure–activity relationships · X-ray diffraction

both the solid and solution states and causing a split of the phthalocyanine  $\alpha$  protons in the  $^1\text{H}$  NMR spectra that is significantly different from all SiPcs reported so far. The remarkable photostability, good singlet oxygen quantum yield, and efficient in vitro photodynamic activity synergistically show that compound **3** is one of the most promising photosensitizers for PDT.

## Introduction

As a multifunctional dye, phthalocyanine (Pc) has received great attention for applications in numerous areas, such as pigments,<sup>[1]</sup> catalysts,<sup>[2]</sup> photoconducting agents,<sup>[3]</sup> chemical sensors,<sup>[4]</sup> optical storage materials,<sup>[5]</sup> photovoltaic cells,<sup>[6]</sup> organic semiconductors,<sup>[6c,7]</sup> and photodynamic therapy<sup>[8]</sup> (PDT) of cancer. Among these applications, the use of Pcs as photosensitizers for PDT has attracted much more attention in recent decades because of their efficient singlet oxygen generation and intense absorption in the red and near-IR (NIR) region that is recognized to be the optimal therapeutic window with high tissue penetration for treatment of deep-seated tumors. For this strategy, a variety of Pcs with different functionalities and central ions have been developed to evaluate their photophysical and biological properties. So far, silicon phthalocyanine (SiPc) is one of the most efficient Pc-based photosensitizers, owing to its efficient photoactivity and biocompatibility.<sup>[9]</sup>

The axial functionalities of SiPc greatly reduce aggregation caused by the large  $\pi$ -conjugated system, and thus, increase the photosensitizing efficiency dramatically.<sup>[10]</sup> For example, unsymmetrical Pc **4** (see Scheme 1 below) is one of the few photosensitizers that has been used in preclinical trials.<sup>[11]</sup> However, the stability and photophysical and PDT

activities of SiPc are greatly affected by the nature of the axial ligands. In particular, the bond between silicon and the axial ligands is often the most fragile part of the SiPc, resulting in unpredictable changes to the molecular structure and photophysical properties. For example, Ng et al. reported that a ligand-exchange reaction occurred during the recrystallization of axial 1,3-bis(dimethylamino)-2-propoxy-substituted SiPc in MeOH/ $\text{CHCl}_3$ .<sup>[12]</sup> Kenney et al. found that the axial Si–Me bonds could be photolyzed easily in the presence of  $\text{H}_2\text{O}$  to give Si–OH.<sup>[9a]</sup>

Herein, a series of axially substituted SiPcs have been synthesized. With changes to the axial ligands, their stability, photophysical and PDT activities, and the reactivity of axial ligand upon shielding by the Pc ring current were compared and evaluated for the first time. In addition, the effect of the axial ligand on the molecular configuration of SiPc was revealed simultaneously by single-crystal XRD analysis and temperature-dependent  $^1\text{H}$  NMR spectroscopy. By studying this series of structurally related compounds, the structure–activity relationships are demonstrated directly.

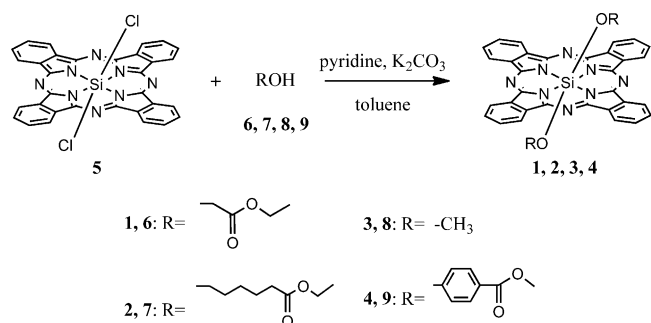
## Results and Discussion

### Synthesis and Characterization

The most straightforward preparation of axially substituted SiPc is the treatment of commercially available silicon phthalocyanine dichloride (**5**) with the relevant alcohol in the presence of a base (Scheme 1).<sup>[13]</sup> Compound **4** was synthesized previously with pyridine as the organic base.<sup>[14]</sup> According to this published procedure, herein, compound **5** was first reacted with the corresponding alcohols in the presence of pyridine in toluene at reflux for 2–3 days to give

[a] L. Luan, L. Ding, J. Shi, W. Fang, Y. Ni, Prof. W. Liu  
State Key Laboratory of Crystal Materials  
Shandong University, Jinan  
250100 Shandong (P.R. China)  
E-mail: weiliu@sdu.edu.cn

Supporting information for this article is available on the WWW under <http://dx.doi.org/10.1002/asia.201402813>.



Scheme 1. Synthetic route to the Pc compounds described herein by treating **5** with ethyl glycolate (**6**), ethyl 6-hydroxyhexanoate (**7**), methanol (**8**), or methyl 4-hydroxybenzoate (**9**).

**SiPcs 1–3.** We found that the reaction, however, could be accelerated greatly through the addition of anhydrous  $K_2CO_3$ . As a result, SiPc **1–4** could be synthesized in high yield within 6 h and pure products were obtained through simple recrystallization; Pc **3** was synthesized previously by using a different procedure before.<sup>[15]</sup> All the new compounds were fully characterized by UV/Vis absorption,  $^1H$  and  $^{13}C$  NMR spectroscopy, IR spectroscopy, mass spectrometry, and elemental analysis. Compounds **1** and **3** were also characterized structurally by single-crystal XRD analysis.

In the  $^1H$  NMR spectra, the macrocyclic protons for all these compounds appear as characteristic signals of unsubstituted Pcs, showing two AA'BB' patterns at  $\delta = 8–10$  ppm, which correspond to the  $\alpha$  and  $\beta$  protons of the Pc ring. Owing to shielding of the macrocyclic diamagnetic ring currents, the signals for the axial ligands appear at very upfield positions relative to the corresponding free ligands, which is also common for axially substituted metal Pcs, such as ruthenium,<sup>[16]</sup> gallium,<sup>[17]</sup> and indium<sup>[18]</sup> Pcs. In addition, the chemical shifts follow the order of  $-O(CH_2)_5COOEt > -OCH_3 > -OCH_2COOEt > -OC_6H_4COOMe$ , which is in agreement with the electron-donating abilities of the ligands.

Compound **2** decomposed gradually within several hours in  $CDCl_3$  and the  $^1H$  NMR spectrum was obtained by using fresh prepared solutions that were scanned immediately. On the contrary, compound **2** is stable enough in  $CHCl_3$  and the reasons for this phenomenon remain elusive to us at this stage. In addition, the poor solubility of **3** inhibits us from obtaining a clearly resolved  $^{13}C$  NMR spectrum.

Interestingly, splitting of the Pc  $\alpha$  protons of **3** was observed in the  $^1H$  NMR spectrum, and the ratio of the two components was dependent on temperature (Figure 1). At 295 K, the  $^1H$  NMR spectrum exhibited two clearly resolved signals at  $\delta \approx 9.68$  and 9.58 ppm. Increasing the temperature from 295 to 325 K resulted in merging of the signal at  $\delta = 9.58$  ppm into the one at  $\delta = 9.68$  ppm. In addition, temperature-dependent splitting of the methyl proton signal was also observed. However, it is much less clear than that of the  $\alpha$  protons. At 295 K, only a slight shoulder could be seen for the signal of  $\delta = -1.78$  ppm (Figure 1). In contrast, no such phenomenon was observed for the other SiPcs.

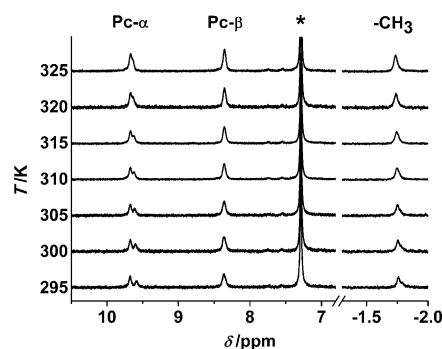
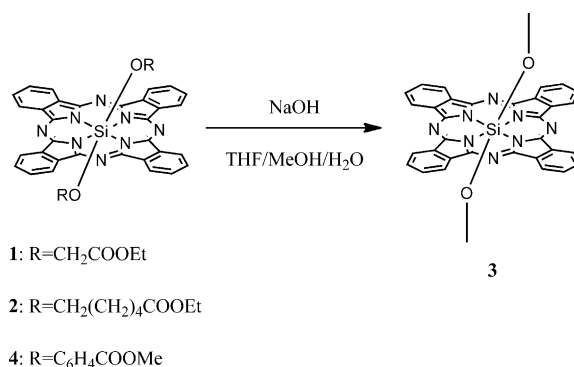


Figure 1.  $^1H$  NMR spectra of **3** in  $CDCl_3$  at different temperatures.

Therefore, we believe that the axial  $-OMe$  group should account for such splitting of the Pc  $\alpha$  protons.

In the high-resolution ESI mass spectra of SiPcs **1–4**, two set of peaks corresponding to  $[M+H]^+$  and  $[M+Na]^+$  were observed. Unlike other metal Pcs, the molecular ion peak accounting for the molecular weight after the removal one of the axial ligands (R) from the SiPc, namely,  $[M-R]^+$ , was always observed for **1–4** in the MALDI-TOF mass spectra; this showed that cleavage occurred of the Si–O bond, which was susceptible under the MS conditions.

To evaluate the Pc shielding effect on the reactivity of the axial ligand, SiPcs **1**, **2**, and **4** were hydrolyzed by using NaOH at 45 °C in a mixed solvent system of tetrahydrofuran (THF)/MeOH/ $H_2O$  according to a method described by us previously.<sup>[19]</sup> However, both compounds **1** and **2** underwent a ligand-exchange reaction with MeOH, which resulted in the formation of methoxy-substituted SiPc **3** instead of the hydrolyzed SiPcs with COONa (Scheme 2). In contrast,



Scheme 2. The hydrolysis of compounds **1**, **2**, and **4**.

compound **4** remained intact under the same conditions, which showed that the stronger electron-accepting ability of  $-OC_6H_4COOMe$  strengthened the Si–O bond. Upon further elevating the temperature to 90 °C, compound **4** went through the same ligand-exchange reaction again to give **3** as the final product without the formation of any hydrolyzed product. If the Si–O bonds in **1** and **2** are weaker than those of an ester, inducing a ligand-exchange reaction before hydrolysis at 45 °C, the intactness of **4** under the same condi-

tions shows that the ester groups are still robust enough to resist hydrolysis in the presence of the Si–O bond. In contrast, the same functional group of **4** could be easily hydrolyzed at 45 °C under the same conditions when it was attached at the peripheral position of Pc.<sup>[19a]</sup> The reactivity of the ester group is greatly passivated by the shielding effect of the Pc ring. Kobayashi et al. reported that the hydrolysis of ester groups in dendrimer SiPcs proceeded successfully in an aqueous solution of KOH.<sup>[20]</sup> Considering the long spacer between the silicon atom and the terminal esters, the shielding effect of Pc should be negligible and the reactivity of ester groups should not be affected.

### Electronic Absorption and Photophysical Properties

All absorption and photophysical property measurements were conducted in *N,N*-dimethylformamide (DMF). The absorption spectra of SiPcs **1–4** give typical UV/Vis absorptions for monomeric Pcs (Figure 2), with a B band at  $\lambda =$

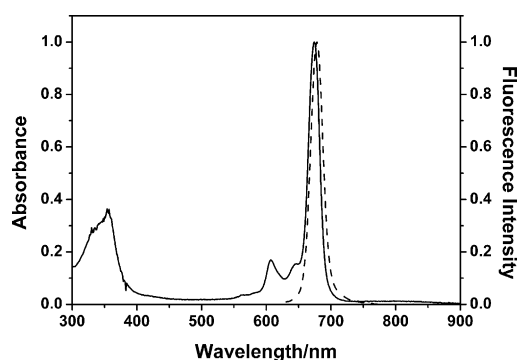


Figure 2. Normalized absorption (—) and emission spectra (---,  $\lambda_{\text{ex}} = 610$  nm) of **1** in DMF.

355 nm and a sharp Q band at  $\lambda = 671\text{--}683$  nm, along with two vibronic bands at  $\lambda = 605\text{--}613$  and  $644\text{--}655$  nm (Table 1). The absorptions for SiPcs **1–3** are very similar; however, a 10 nm redshift could be observed for SiPc **4** as a result of the stronger electron-accepting ability of an aromatic ligand than that of an alkyl ligand. Upon excitation at

Table 1. Electronic absorption and photophysical data for compounds **1–4** in DMF.

	$\lambda$ [nm] (log $\epsilon$ )	$\lambda_{\text{em}}$ [a] [nm]	$\Phi_{\text{F}}$ [b]	$\Phi_{\Delta}$ [c]
<b>1</b>	355(5.00), 607(4.67), 647(4.62), 674(5.44)	678	0.35	0.45
<b>2</b>	355(4.93), 605(4.63), 644(4.58), 673(5.41)	676	0.34	0.48
<b>3</b>	355(4.87), 605(4.54), 646(4.51), 671(5.28)	675	0.46	0.50
<b>4</b>	355(4.97), 613(4.64), 655(4.59), 683(5.36)	687	0.34	0.44

[a] Excited at  $\lambda = 610$  nm. [b] Relative to zinc Pc (ZnPc) in DMF as the reference ( $\Phi_{\text{F}} = 0.28$ ). [c] Relative to ZnPc in DMF as the reference ( $\Phi_{\Delta} = 0.56$ ).

$\lambda = 610$  nm in the same solvent, these SiPcs gave emissions between  $\lambda = 675$  and  $687$  nm with fluorescence quantum yields in the range of 0.34–0.46. SiPcs **1**, **2**, **4** show similar fluorescence quantum yields (0.34–0.35), but the value of **3** is higher at 0.46.

The singlet oxygen quantum yields of SiPcs **1–4** were determined by a steady-state method with 1,3-diphenylisobenzofuran (DPBF) as the quenching agent, according to a method described previously.<sup>[21]</sup> Although compound **4** was reported previously, its biological activities have not yet been evaluated. All of these Pcs produce singlet oxygen efficiently with values in the range of 0.44–0.50 (Table 1), and negligible decomposition was observed during irradiation ( $\lambda > 610$  nm; Figure 3 and Table 1).

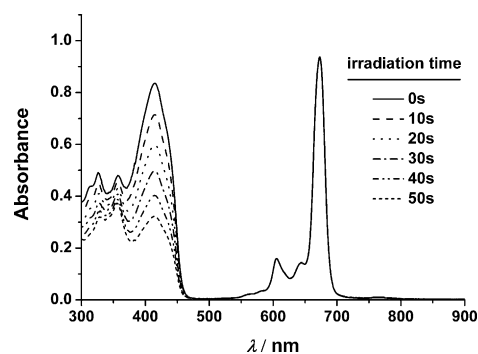


Figure 3. Typical electronic absorption spectra for the determination of the singlet oxygen quantum yield of **2** in DMF exposed to light  $\lambda > 610$  nm.

### Photostability

The photostabilities of these compounds were tested by monitoring the Q-band absorbance decrease over time upon exposure to red light in air. The light intensity used herein ( $\lambda > 610$  nm,  $\approx 1.7$  mWcm<sup>-2</sup>) was about eight times higher than that for singlet oxygen determination. For comparison, ZnPc was also examined synchronously. Upon irradiation, only slight decomposition took place for these SiPcs, especially for SiPc **3**, and no absorbance drop was observed over 60 min. On the contrary, degradation was much more serious for ZnPc under the same conditions: about 60% of ZnPc decomposed within the first 10 min of irradiation (Figure 4). The photodegradation rates follow the order of ZnPc  $\gg$  **1** > **4** > **2** > **3**. Herein, compound **3** is the most stable SiPc to resist photolysis by red light.

### Crystal Structure

Compounds **1** and **3** were characterized structurally by XRD analysis. Single crystals were grown by slow diffusion of hexane into a solution of SiPc **1** or **3** in CHCl<sub>3</sub>. Both single crystals of **1** and **3** belong to the triclinic system with one molecule per unit cell. Figure 5a shows a perspective view of the molecular structure of **1**, in which the silicon atom is hexacoordinated with four Si–N bonds and two Si–

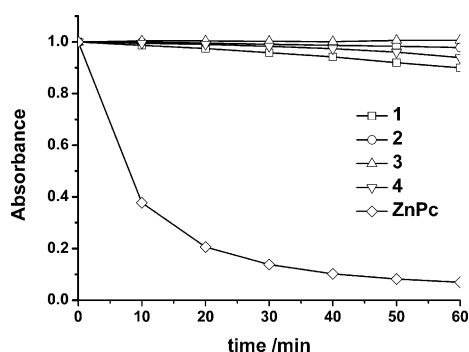


Figure 4. Plots of absorbance at the maximum absorbance wavelength of the Q band in the UV/Vis spectra of **1–4** and ZnPc (ca. 5.0 μM) in DMF upon irradiation with red light ( $\lambda > 610$  nm).

O bonds. The two axial ligands reside at opposite sides of planar Pc with the silicon atom serving as the inversion center. The average bond lengths of Si–O and Si–N are 1.721(2) and 1.916(2) Å, respectively, which are comparable with those of reported SiPcs.<sup>[12]</sup> Similar to compound **1**, the molecular structure of **3** also contains a silicon atom as the inversion center. However, rotation of –Me along with the O–Si–O axis was also observed, which resulted in the two opposite –Me groups deviating from the inversion image with a rotation angle of 62.7(4)° (Figure 5b). The ratio be-

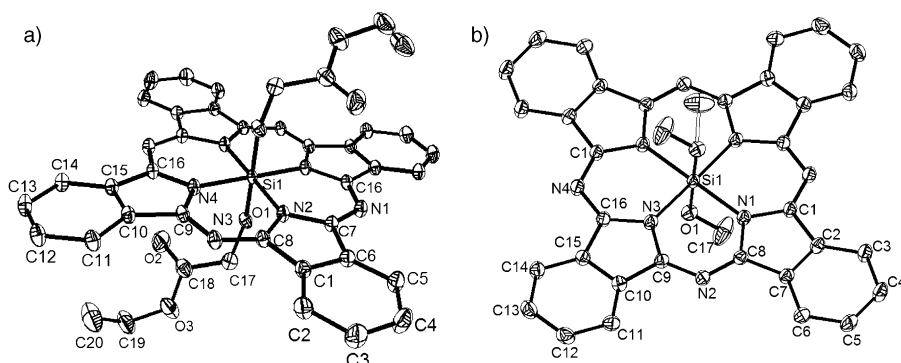


Figure 5. Molecular structures **1** (a) and **3** (b) obtained by single-crystal XRD. Ellipsoids are given at the 30% probability level.

tween the two orientations with or without an inversion center, namely, compounds **3a** and **3b**, is 1.26 at 293 K.

We observed splitting of the Pc  $\alpha$  protons of **3** in the  $^1\text{H}$  NMR spectra, as described above, and expected that it originated from the effect of axial –OMe. The crystal structure results are in agreement with our speculation, and the two molecular orientations should account for splitting of the  $\alpha$  protons. Furthermore, the ratio between the two  $^1\text{H}$  NMR signals at 295 K is about 1.23, which is comparable to the **3a/3b** ratio of 1.26 in the crystal structure at the same temperature; this shows consistency between the molecular configuration and  $^1\text{H}$  NMR spectra. It is not difficult to understand this phenomenon. The small size of –Me enables it to be more agile than the other bulky groups and rotation

occurs for –Me, which results in two orientations simultaneously coexisting in **3**. Upon increasing the temperature, thermodynamically unstable species of **3b**, which, without an inversion center, changes into more stable **3a**, of which the silicon atom serves as the inversion center. Accordingly, the two  $^1\text{H}$  NMR signals for the  $\alpha$  protons merge into one signal, which is attributed to that of **3a**. To the best of our knowledge, except for **3**, the X-ray single-crystal structures of symmetrically substituted SiPcs reported so far have all possessed only one molecular configuration in the crystals, of which the silicon atom serves as the inversion center, similar to that in **1** and **3a**, and no splitting of the  $\alpha$  proton in the  $^1\text{H}$  NMR spectra is observed.<sup>[22]</sup> This further confirms that splitting of the  $\alpha$  proton arises from rotation of –Me in **3**.

Kojima et al. obtained single crystals of **3** by evaporation of a solution in chloroform solution.<sup>[15]</sup> The XRD data showed that the crystal also belonged to the same triclinic  $P\bar{1}$  space group as that in our study.<sup>[15]</sup> However, water molecules were found to coexist with **3** in the single crystal with a molar ratio of one to two, and disorder of the carbon atom of the methoxy group was attributed to water molecules in the crystal lattice. Because no water could be found in the single crystal of this study, thermodynamic rotation of the methyl group should account for the different orientation of **3** observed herein.

### In Vitro Photodynamic Activities

The in vitro photodynamic activities of compounds **1–4** were investigated against two cervical carcinoma cell lines, namely, HeLa and SiHa. Dose-dependent cell viabilities were observed for all of these SiPcs in both cell lines. The  $\text{IC}_{50}$  values, which are defined as the concentration resulting in 50% inhibition of cell proliferation by light treatment, follow the order of  $4 > 2 > 1 > 3$  for both

cell lines (Table 2). As shown in Figure 6, all of these compounds are essentially noncytotoxic in the absence of light. Compounds **1–3** exhibit very high photocytotoxicity upon exposure to the red light used in our study.

Table 2.  $\text{IC}_{50}$  [ $\mu\text{M}$ ] values of compounds **1–4** in HeLa and SiHa cell lines.<sup>[a]</sup>

	<b>1</b>	<b>2</b>	<b>3</b>	<b>4</b>
HeLa	0.422	1.61	0.295	– <sup>[b]</sup>
SiHa	0.629	1.171	0.353	– <sup>[b]</sup>

[a] Irradiated with red light ( $\lambda > 610$  nm). [b] Not determined under the conditions used for phototoxicity measurements.

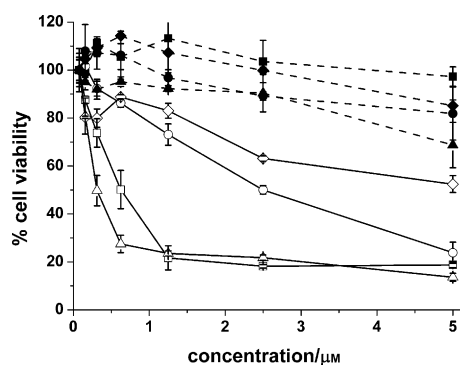


Figure 6. Comparison of the cytotoxic effects of **1** (squares), **2** (circles), **3** (triangles), and **4** (diamonds) on HeLa cells in the absence (solid symbols) and presence (open symbols) of light ( $\lambda > 610$  nm).

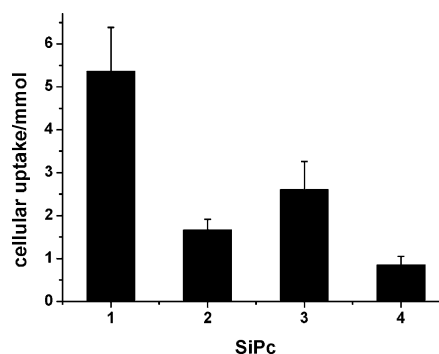


Figure 8. Cellular uptake in HeLa cells of **1–4** determined by an extraction method with DMF as the solvent.

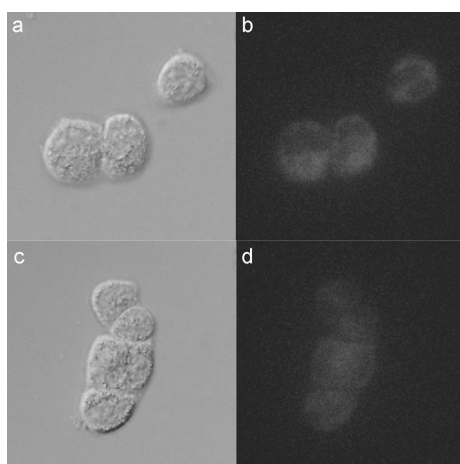


Figure 7. Intracellular localization of **3** (a, b) and **4** (c, d) in HeLa cells incubated at a concentration of  $5 \mu\text{M}$  for 4 h; bright-field (a and c) and fluorescence (b and d) images are shown.

To reveal the different photodynamic activities, intracellular fluorescence microscopy was employed to evaluate the cellular uptake and subcellular localization of these compounds. As shown in Figure 7, these compounds could enter the cells to cause uniform cellular fluorescence in the cytoplasm after incubation for 2 h. The intracellular fluorescence intensities follow the order of  $3 > 1 > 2 > 4$ , which is consistent with the  $\text{IC}_{50}$  values. Because the cellular fluorescence could be affected by either cellular uptake or the extent of aggregation of the photosensitizers, the photosensitizer concentrations inside the cells were quantified by an extraction method. DMF was used to extract the photosensitizers inside the cells after incubation for 4 h. The cellular uptakes of these compounds in HeLa cells are shown in Figure 8. The cellular intake of SiPcs **1**, **2**, and **4** is in good agreement with their phototoxicity. Although compound **3** has a lower uptake than **1**, its higher singlet oxygen quantum yield enables it to be more sensitive during light treatment. As a result, compound **3** is the most effective photosensitizer for PDT.

## Conclusion

A series of axially substituted SiPcs were synthesized with different axial ligands. The reactivity of the axial ligand was greatly passivated by the shielding effect of the Pc ring, and a stronger electron-accepting ability of the axial ligand could strengthen the Si–O bond. Rotation of the axial –OMe ligands of **3** was observed, which resulted in two molecular configurations coexisting synchronously and causing a split of the Pc  $\alpha$  protons in the  $^1\text{H}$  NMR spectra as a result of the small size of the axial ligand. The remarkable photostability, good singlet oxygen quantum yield, and efficient in vitro photodynamic activity synergistically showed that compound **3** was one of the most promising photosensitizers for PDT.

## Experimental Section

### Materials and Methods

All reactions were performed under a nitrogen atmosphere. Pyridine, toluene, and methanol were distilled from calcium hydride, sodium, and calcium hydride, respectively. All other solvents and reagents were of reagent grade and were used as received.

$^1\text{H}$  and  $^{13}\text{C}$  NMR spectra were recorded on a Bruker AVANCE 300 MHz spectrometer ( $^1\text{H}$ , 300;  $^{13}\text{C}$ , 75.4 MHz) in  $\text{CDCl}_3$ . Spectra were referenced internally to the residual solvent signal of  $\text{CDCl}_3$  ( $^1\text{H}$ :  $\delta = 7.26$  ppm;  $^{13}\text{C}$ :  $\delta = 77.0$  ppm) or relative to  $\text{SiMe}_4$  ( $\delta = 0$  ppm). HRMS (ESI) results were recorded on an Agilent G6410 Triple Quadrupole mass spectrometer. IR spectra were recorded on a Thermo NEXUS 670 IR spectrometer. The 3-(4,5-dimethylthiazol-2-yl)-2,5-diphenyltetrazolium bromide (MTT) assay was performed on a Bio-TEK ELX 800 microplate reader.

UV/Vis and steady-state fluorescence spectra were recorded on a PerkinElmer Lambda-35 UV/Vis spectrometer and a Hitachi F-4500 fluorescence spectrometer, respectively. The fluorescence quantum yields ( $\Phi_{\text{F}}$ ) were determined by following a previously reported method with ZnPc as the reference ( $\Phi_{\text{F}} = 0.28$  in DMF).<sup>[21]</sup> To minimize reabsorption of radiation by the ground state species, the emission spectra were obtained in very dilute solutions at concentration of about  $5 \times 10^{-7}$  M. The singlet oxygen quantum yields ( $\Phi_{\Delta}$ ) were measured in DMF by the chemical quenching of DPBF with ZnPc as a reference ( $\Phi_{\Delta} = 0.56$ ).<sup>[21,23]</sup>

### Synthesis of Pc **1**

A mixture of **5** (0.056 g, 0.092 mmol), **6** (90  $\mu\text{L}$ , 0.95 mmol),  $\text{K}_2\text{CO}_3$  (0.05 g, 0.36 mmol), and pyridine (1 mL) in toluene (15 mL) was heated at reflux for 6 h. After evaporating the solvent in vacuo, the residue was

redissolved in  $\text{CHCl}_3$  (60 mL). After filtration, the filtrate was concentrated under reduced pressure. The crude product was recrystallized from *n*-hexane to give **1** as a green solid (0.042 g, 61%).  $^1\text{H NMR}$ :  $\delta$  = 9.65–9.67 (m, 8H; Pc-H<sub>a</sub>), 8.34–8.37 (m, 8H; Pc-H<sub>b</sub>), 2.75 (q,  $J$  = 7.2 Hz, 4H; CH<sub>2</sub>), 0.30 (t,  $J$  = 7.2 Hz, 6H; CH<sub>3</sub>), –1.13 ppm (s, 4H; CH<sub>2</sub>);  $^{13}\text{C NMR}$ :  $\delta$  = 209.6, 149.7, 135.9, 131.0, 123.7, 59.2, 55.1, 12.9 ppm; HRMS (ESI):  $m/z$  calcd for  $\text{C}_{40}\text{H}_{30}\text{N}_8\text{O}_6\text{Si}$ : 747.2130 [ $M+H$ ]<sup>+</sup>; found: 747.2149; FTIR (solid, transmission < 92%):  $\tilde{\nu}$  = 665, 700, 728, 759, 777, 806, 830, 871, 911, 1025, 1077, 1118, 1163, 1192, 1289, 1334, 1376, 1427, 1442, 1472, 1520, 1611, 1751, 1980, 2189, 2421, 2581, 2900  $\text{cm}^{-1}$ ; elemental analysis calcd (%) for  $\text{C}_{40}\text{H}_{30}\text{N}_8\text{O}_6\text{Si} \cdot 0.5\text{H}_2\text{O}$ : C 63.56, H 4.13, N 14.83; found: C 63.48, H 4.08, N 14.95.

#### Synthesis of Pc 2

A mixture of **5** (0.057 g, 0.093 mmol), **7** (91  $\mu\text{L}$ , 0.56 mmol),  $\text{K}_2\text{CO}_3$  (0.10 g, 0.75 mmol), and pyridine (1 mL) in toluene (15 mL) was heated at reflux for 6 h. After evaporating the solvent in vacuo, the residue was redissolved in  $\text{CHCl}_3$  (50 mL). After filtration, the filtrate was concentrated under reduced pressure. The crude product was recrystallized from *n*-hexane to give **2** as a green solid (0.059 g, 73%).  $^1\text{H NMR}$ :  $\delta$  = 9.60–9.66 (m, 8H; Pc-H<sub>a</sub>), 8.27–8.36 (m, 8H; Pc-H<sub>b</sub>), 3.79 (q,  $J$  = 7.2 Hz, 4H; CH<sub>2</sub>), 1.19 (t,  $J$  = 5.4 Hz, 4H; CH<sub>2</sub>), 1.01 (t,  $J$  = 7.2 Hz, 6H; CH<sub>3</sub>), –0.06 (quint,  $J$  = 7.8 Hz, 4H; CH<sub>2</sub>), –1.37 to –1.47 (m, 4H; CH<sub>2</sub>), –1.66 (quint,  $J$  = 6.6 Hz, 4H; CH<sub>2</sub>), –2.11 ppm (t,  $J$  = 6.0 Hz, 4H; CH<sub>2</sub>);  $^{13}\text{C NMR}$ :  $\delta$  = 164.4, 149.7, 136.0, 130.7, 123.5, 62.7, 60.6, 34.3, 32.3, 25.3, 24.6, 14.2 ppm; HRMS (ESI):  $m/z$  calcd for  $\text{C}_{48}\text{H}_{46}\text{N}_8\text{O}_6\text{Si}$ : 859.3382 [ $M+H$ ]<sup>+</sup>; found: 859.3374; FTIR (solid, transmission < 92%):  $\tilde{\nu}$  = 732, 759, 813, 861, 910, 1025, 1036, 1080, 1101, 1121, 1165, 1208, 1270, 1290, 1305, 1334, 1352, 1368, 1428, 1456, 1472, 1520, 1614, 1721, 1980, 2197, 2270, 2420, 2589, 2632, 2673, 2861, 2924, 2974, 3062  $\text{cm}^{-1}$ ; elemental analysis calcd (%) for  $\text{C}_{48}\text{H}_{46}\text{N}_8\text{O}_6\text{Si}$ : C 67.11, H 5.40, N 13.04; found: C 67.4, H 5.40, N 12.89.

#### Synthesis of Pc 3

A mixture of **5** (0.054 g, 0.089 mmol), **8** (300  $\mu\text{L}$ , 7.41 mmol),  $\text{K}_2\text{CO}_3$  (0.11 g, 0.77 mmol), and pyridine (1 mL) in toluene (15 mL) was heated at reflux for 6 h. After evaporating the solvent in vacuo, the residue was dissolved in  $\text{CHCl}_3$  (100 mL). After filtration, the filtrate was concentrated under reduced pressure to give **3** as a dark-green solid.  $^1\text{H NMR}$ :  $\delta$  = 9.68–9.58 (brs, 8H; Pc-H<sub>a</sub>), 8.34 (brs, 8H; Pc-H<sub>b</sub>), –1.78 ppm (brs, 6H; CH<sub>3</sub>); HRMS (ESI):  $m/z$  calcd for  $\text{C}_{34}\text{H}_{22}\text{N}_8\text{O}_2\text{Si}$ : 603.1708 [ $M+H$ ]<sup>+</sup>; found: 603.1708; FTIR (solid, transmission < 92%):  $\tilde{\nu}$  = 726, 758, 778, 831, 909, 951, 1076, 1094, 1121, 1163, 1184, 1288, 1332, 1351, 1429, 1471, 1518, 1611, 1721, 2184, 2582, 2810, 2918, 3485  $\text{cm}^{-1}$ ; elemental analysis calcd (%) for  $\text{C}_{34}\text{H}_{22}\text{N}_8\text{O}_2\text{Si}$ : C 67.76, H 3.68, N 18.59; found: C 67.80, H 3.68, N 18.64.

#### Synthesis of Pc 4<sup>[14]</sup>

A mixture of **5** (0.234 g, 0.383 mmol), **9** (0.369 g, 2.43 mmol),  $\text{K}_2\text{CO}_3$  (0.41 g, 2.97 mmol), and pyridine (1.4 mL) in toluene (20 mL) was heated at reflux for 6 h. After evaporating the solvent in vacuo, the residue was redissolved in  $\text{CHCl}_3$  (100 mL). After filtration, the filtrate was evaporated under reduced pressure. The crude product was recrystallized from methanol to give **4** as a blue solid (0.20 g, 62%).  $^1\text{H NMR}$ :  $\delta$  = 9.63–9.65 (m, 8H; Pc-H<sub>a</sub>), 8.37–8.40 (m, 8H; Pc-H<sub>b</sub>), 6.30 (dd,  $J$  = 2.1, 6.9 Hz, 4H; ArH), 3.43 (s, 6H; CH<sub>3</sub>), 2.45 ppm (dd,  $J$  = 1.8, 6.9 Hz, 4H; ArH);  $^{13}\text{C NMR}$ :  $\delta$  = 149.7, 135.4, 131.9, 131.4, 129.2, 123.9, 117.3, 115.1, 51.9 ppm; HRMS (ESI):  $m/z$  calcd for  $\text{C}_{48}\text{H}_{30}\text{N}_8\text{O}_6\text{Si}$ : 843.2130 [ $M+H$ ]<sup>+</sup>; found: 843.2122; FTIR (solid, transmission < 92%):  $\tilde{\nu}$  = 701, 727, 760, 774, 819, 860, 885, 912, 961, 1010, 1079, 1097, 1112, 1124, 1158, 1187, 1266, 1287, 1335, 1352, 1429, 1474, 1504, 1525, 1568, 1596, 1718, 1776, 2430, 2583, 2681, 2892, 2950, 3021  $\text{cm}^{-1}$ ; elemental analysis calcd (%) for  $\text{C}_{48}\text{H}_{30}\text{N}_8\text{O}_6\text{Si}$ : C 68.4, H 3.59, N 13.29; found: C 68.61, H 3.58, N 13.31.

#### Cell Lines and Culture Conditions

The HeLa cells were maintained in Dulbecco's modified Eagle's medium (DMEM; HyClone, no. SH30022.01B) supplemented with calf serum (10%) and penicillin/streptomycin (100 units  $\text{mL}^{-1}$  and 100  $\mu\text{g mL}^{-1}$ , respectively). The SiHa cells were maintained under the same conditions as

those used for the HeLa cells. Approximately  $3 \times 10^5$  cells per dish (3.5 cm) or 5000 cells per well in 96-well plates were incubated at 37°C in a humidified 5%  $\text{CO}_2$  atmosphere.

#### Cellular Uptake Studies

Pcs **1–4** were first dissolved in DMSO to give  $5.0 \times 10^{-4}$  M solutions, which were diluted to the appropriate concentrations with culture medium containing 1% (v/v) Cremophor EL. The cells, after being rinsed with phosphate buffered saline (PBS), were incubated with these Pc solutions (1 mL) for 4 h in a 3.5 cm dish. The medium was removed and the cells were then rinsed twice with PBS, digested by trypsin, and refilled with the culture medium (500  $\mu\text{L}$ ). After removing the medium, the freeze-dried cells were extracted with DMF (500  $\mu\text{L}$ ). The UV/Vis absorption spectra were measured to determine the concentrations of the photosensitizers.

#### Photocytotoxicity Assays

Pcs **1–4** were first dissolved in DMSO to give  $5.0 \times 10^{-4}$  M solutions, which were diluted to the appropriate concentrations with culture medium containing 1% (v/v) Cremophor EL. The cells, after being rinsed with PBS, were incubated with these Pc solutions (100  $\mu\text{L}$ ) for 4 h at 37°C in a 96-well plate. The cells were then rinsed twice with PBS and refilled with the culture medium (100  $\mu\text{L}$ ) before being illuminated at ambient temperature. The light source consisted of a 150 W halogen lamp, a water tank for cooling, and a color glass filter (Newport; cut-on  $\lambda$  = 610 nm). The fluence rate ( $\lambda$  > 610 nm) was about 2.8  $\text{J cm}^{-2}$  within 20 min. Cell viability was determined by means of the colorimetric MTT assay.

#### Intracellular Fluorescence Studies

HeLa or SiHa cells in the culture medium (1.5 mL) were seeded on a coverslip and incubated overnight at 37°C under 5%  $\text{CO}_2$ . After removing the medium, the cells were incubated with a solution of **1**, **2**, **3**, or **4** in the medium (5  $\mu\text{M}$ , 1.5 mL) for 2 h. The cells were then rinsed with PBS and viewed with an Olympus IX71 inverted microscope equipped with a U-MWU2 fluorescence unit, excited at  $\lambda$  = 330–380 nm and monitored at  $\lambda$  > 420 nm, and intracellular fluorescence images were captured.

#### Crystallographic XRD Analysis

The single-crystal XRD data were obtained at room temperature (293 K) by using a Bruker SMART-II equipped with charge-coupled area-detector diffractometer with graphite-monochromated  $\text{MoK}\alpha$  radiation ( $\lambda$  = 0.71073 Å). All structures were solved by direct methods and refined by full-matrix least-squares technique on  $F^2$  by using the SHELX programs. Details are given in Table 3.

CCDC 1027604 (**1**) and 1027605 (**3**) contain the supplementary crystallographic data for this paper. These data can be obtained free of charge from The Cambridge Crystallographic Data Centre via [www.ccdc.cam.ac.uk/data\\_request/cif](http://www.ccdc.cam.ac.uk/data_request/cif).

## Acknowledgements

This work was supported by grants from the Natural Science Foundation of China (21071090) and the Excellent Young Scientist Fund of Shandong Province (BS2010L032). We also acknowledge financial support from the Research Fund for the Doctoral Program of Higher Education of China (20100131120026) and Independent Innovation Foundation of Shandong University (2012JJC013).

- [1] *Phthalocyanines, Properties and Applications*, vols 1–4 (Eds: C. C. Leznoff, A. B. P. Lever), VCH, Weinheim, New York, **1989–1996**.
- [2] a) Z. F. Huang, H. W. Bao, Y. Y. Yao, W. Y. Lu, W. X. Chen, *Appl. Catal. B* **2014**, *154*, 36–43; b) T. Abe, N. Taira, Y. Tanno, Y. Kikuchi, K. Nagai, *Chem. Commun.* **2014**, *50*, 1950–1952; c) J. Masa, W. Schuhmann, *Chem. Eur. J.* **2013**, *19*, 9644–9654; d) C. Ruiguo, R.

Table 3. Crystallographic data for SiPcs **1** and **3**.

	<b>1</b>	<b>3</b>
formula	C <sub>40</sub> H <sub>28</sub> N <sub>8</sub> O <sub>6</sub> Si	C <sub>34</sub> H <sub>22</sub> N <sub>8</sub> O <sub>2</sub> Si
M <sub>w</sub>	744.79	602.69
T [K]	293(2)	293(2)
λ [Å]	0.71073	0.71069
crystal system, space group	triclinic, P $\bar{1}$	triclinic, P $\bar{1}$
a [Å]	8.6434(11)	7.4720(9)
b [Å]	10.0699(15)	8.3144(10)
c [Å]	11.1386(15)	11.6175(14)
α [°]	110.4690(10)	75.3957(14)
β [°]	103.2350(10)	74.9915(14)
γ [°]	101.8120(10)	83.7316(15)
Z	1	1
ρ <sub>calcd</sub> [mg m <sup>-3</sup> ]	1.472	1.485
μ [mm <sup>-1</sup> ]	0.136	0.139
F(000)	386	312
crystal size [mm]	0.48 × 0.26 × 0.24	0.38 × 0.27 × 0.02
θ range for data collection [°]	2.07 to 27.54	1.87 to 27.51
reflms collected/unique	9777/3805 [R(int) = 0.0185]	7949/3056 [R(int) = 0.0261]
completeness to θ = 27.51 [%]	98.1	98.4
absorption correction	semiempirical from equivalents	semiempirical from equivalents
max/min transmission	0.9682/0.9378	0.9972/0.9491
data/restraints/parameters	3805/0/251	3056/0/215
goodness-of-fit on F <sup>2</sup>	1.066	0.977
final R indices [I > 2σ(I)]	R1 = 0.0747 wR2 = 0.2258	R1 = 0.0438 wR2 = 0.1174
R indices (all data)	R1 = 0.0839 wR2 = 0.2371	R1 = 0.0607 wR2 = 0.1280
largest difference peak/hole [e Å <sup>-3</sup> ]	1.585/−0.510	0.547/−0.296

Thapa, K. Hyejung, X. Xiaodong, K. Min Gyu, L. Qing, P. Noejung, L. Meilin, C. Jaephil, *Nat. Commun.* **2013**, *4*, 2076–2077.

[3] A. Shimada, M. Anzai, A. Kakuta, T. Kawanishi, *IEEE Trans. Ind. Appl.* **1987**, *IA-23*, 804–809.

[4] a) G. Guillaud, J. Simon, J. P. Germain, *Coord. Chem. Rev.* **1998**, *178*, 1433–1484; b) B. Wang, Y. Q. Wu, X. L. Wang, Z. M. Chen, C. Y. He, *Sens. Actuators B* **2014**, *190*, 157–164.

[5] P. Gregory, *J. Porphyrins Phthalocyanines* **2000**, *4*, 432–437.

[6] a) P. Peumans, S. R. Forrest, *Appl. Phys. Lett.* **2001**, *79*, 126–128; b) C. W. Tang, *Appl. Phys. Lett.* **1986**, *48*, 183–185; c) P. Peumans, S. Uchida, S. R. Forrest, *Nature* **2003**, *425*, 158–162.

[7] a) J. Z. Jiang, D. K. P. Ng, *Acc. Chem. Res.* **2009**, *42*, 79–88; b) G. Horowitz, *Adv. Mater.* **1998**, *10*, 365–377.

[8] a) I. J. MacDonald, T. J. Dougherty, *J. Porphyrins Phthalocyanines* **2001**, *5*, 105–129; b) M. C. DeRosa, R. J. Crutchley, *Coord. Chem. Rev.* **2002**, *233*, 351–371; c) M. Ochsner, *J. Photochem. Photobiol. B*

**1997**, *39*, 1–18; d) J. T. F. Lau, P.-C. Lo, X.-J. Jiang, Q. Wang, D. K. P. Ng, *J. Med. Chem.* **2014**, *57*, 4088–4097; e) M. R. Ke, D. K. P. Ng, P. C. Lo, *Chem. Asian J.* **2014**, *9*, 554–561; f) X. W. Chen, M. R. Ke, X. S. Li, W. L. Lan, M. F. Zhang, J. D. Huang, *Chem. Asian J.* **2013**, *8*, 3063–3070.

[9] a) N. L. Oleinick, A. R. Antunez, M. E. Clay, B. D. Rihter, M. E. Kenney, *Photochem. Photobiol.* **1993**, *57*, 242–247; b) W. Rodríguez-Córdoba, R. Noria, C. A. Guarín, J. Peon, *J. Am. Chem. Soc.* **2011**, *133*, 4698–4701; c) M. E. El-Khouly, J. H. Kim, K.-Y. Kay, C. S. Choi, O. Ito, S. Fukuzumi, *Chem. Eur. J.* **2009**, *15*, 5301–5310.

[10] F. J. Céspedes-Guirao, L. Martín-Gomis, K. Ohkubo, S. Fukuzumi, F. Fernández-Lázaro, Á. Sastre-Santos, *Chem. Eur. J.* **2011**, *17*, 9153–9163.

[11] M. Lam, A. H. Hsia, Y. Liu, M. Guo, A. R. Swick, J. C. Berlin, T. S. McCormick, M. E. Kenney, N. L. Oleinick, K. D. Cooper, E. D. Baron, *Clin. Exp. Dermatol.* **2011**, *36*, 645–651.

[12] P. C. Lo, J. D. Huang, D. Y. Y. Cheng, E. Y. M. Chan, W. P. Fong, W. H. Ko, D. K. P. Ng, *Chem. Eur. J.* **2004**, *10*, 4831–4838.

[13] M. E. El-Khouly, E. S. Kang, K.-Y. Kay, C. S. Choi, Y. Aaraki, O. Ito, *Chem. Eur. J.* **2007**, *13*, 2854–2863.

[14] J.-Y. Liu, E. A. Ermilov, B. Roder, D. K. P. Ng, *Chem. Commun.* **2009**, 1517–1519.

[15] Y. Kojima, Y. T. Osano, T. Ohashi, *Bull. Chem. Soc. Jpn.* **2000**, *73*, 2469–2475.

[16] T. Rawling, A. M. McDonagh, S. B. Colbran, *Inorg. Chim. Acta* **2008**, *361*, 49–55.

[17] a) Y. Chen, S. O'Flaherty, M. Fujitsuka, M. Hanack, L. R. Subramanian, O. Ito, W. J. Blau, *Chem. Mater.* **2002**, *14*, 5163–5168; b) Y. Chen, M. Hanack, Y. Araki, O. Ito, *Chem. Soc. Rev.* **2005**, *34*, 517–529.

[18] M. Hanack, T. Schneider, M. Barthel, J. S. Shirk, S. R. Flom, R. G. S. Pong, *Coord. Chem. Rev.* **2001**, *219*, 235–258.

[19] a) L. Luan, L. Ding, W. Zhang, J. Shi, X. Yu, W. Liu, *Bioorg. Med. Chem. Lett.* **2013**, *23*, 3775–3779; b) L. Luan, J. Chen, L. Ding, J. Wang, X. Cheng, Q. Ren, W. Liu, *Chem. Lett.* **2012**, *41*, 1012–1014.

[20] T. Uchiyama, K. Ishii, T. Nonomura, N. Kobayashi, S. Isoda, *Chem. Eur. J.* **2003**, *9*, 5757–5761.

[21] A. Ogunsipe, J.-Y. Chen, T. Nyokong, *New J. Chem.* **2004**, *28*, 822–827.

[22] a) M. Brewis, G. J. Clarkson, V. Goddard, M. Helliwell, A. M. Holder, N. B. McKeown, *Angew. Chem. Int. Ed.* **1998**, *37*, 1092–1094; *Angew. Chem.* **1998**, *110*, 1185–1187; b) C. Farren, S. FitzGerald, M. R. Bryce, A. Beeby, A. S. Batsanov, *J. Chem. Soc. Perkin Trans. 2* **2002**, 59–66; c) N. Kobayashi, F. Furuya, G.-C. Yug, H. Wakita, M. Yokomizo, N. Ishikawa, *Chem. Eur. J.* **2002**, *8*, 1474–1484; d) X. Leng, D. K. P. Ng, *Eur. J. Inorg. Chem.* **2007**, 4615–4620; e) X.-M. Shen, X.-J. Jiang, C.-C. Huang, H.-H. Zhang, J.-D. Huang, *Tetrahedron* **2010**, *66*, 9041–9048; f) J. L. Sosa-Sánchez, A. Sosa-Sánchez, N. Farfán, L. S. Zamudio-Rivera, G. López-Mendoza, J. Pérez Flores, H. I. Beltrán, *Chem. Eur. J.* **2005**, *11*, 4263–4273.

[23] I. Seotsanyana-Mokhosi, N. Kuznetsova, T. Nyokong, *J. Photochem. Photobiol. A* **2001**, *140*, 215–222.

Received: July 10, 2014  
Revised: August 8, 2014  
Published online: October 9, 2014